#158

Papers from the GEOPHYSICAL LABORATORY
Carnegie Institution of Washington NO. 2339

Physica C 208 (1993) 277–285
North-Holland

PHYSICA C

High pressure structural phase transitions in the organic superconductor κ-$(ET)_2Cu[N(CN)_2]Cl$

A.J. Schultz, U. Geiser, H.H. Wang and J.M. Williams
Chemistry and Materials Science Divisions, Argonne National Laboratory, Argonne, IL 60439, USA

L.W. Finger and R.M. Hazen
Geophysical Laboratory and Center for High Pressure Research, Carnegie Institution of Washington, 5251 Broad Branch Road NW, Washington, DC 20015, USA

Received 2 February 1993

A reversible symmetry-lowering structural phase transition is observed by X-ray diffraction techniques from single crystals of κ-$(ET)_2Cu[N(CN)_2]Cl$ (ET, or BEDT-TTF, is bis(ethylenedithio)tetrathiafulvalene, $C_{10}H_8S_8$) under applied pressure. At room temperature, by use of a diamond anvil cell, a transition above 8 kbar characterized by peak broadening begins to occur. The transition is also observed by cooling crystals coated with Apiezon N vacuum grease, which is a technique that is also used to produce the high pressure superconducting state (T_c=12.8 K, P=0.3 kbar). Given the anisotropic nature of the structure, the ambient pressure linear compressibilities are surprisingly isotropic, with values of $\beta_a=2.39(8)\times10^{-3}$, $\beta_b=2.47(7)\times10^{-3}$, $\beta_c=2.29(9)\times10^{-3}$ kbar^{-1}. At 3 kbar and room temperature, from a complete structure analysis it is shown that the ET molecule conformation is the same as that at ambient pressure although S···S contacts are reduced by as much as 0.05 Å. A second transition, characterized by reversible disappearance of Bragg intensities consistent with pressure-induced amorphization, was observed between 11.4 and 11.8 kbar.

1. Introduction

The κ-phase salts of ET (ET, or BEDT-TTF, is bis(ethylenedithio)tetrathiafulvalene, $C_{10}H_8S_8$) (scheme 1) with copper dicyanamide halide anions have the highest critical temperatures (T_c) for radical-cation-based organic superconductors [1,2]. The bromide analog, κ-$(ET)_2Cu[N(CN)_2]Br$ has the highest T_c at ambient pressure with T_c=11.6 K [3]. The isostructural chloride salt analog, κ-$(ET)_2Cu[N(CN)_2]Cl$, requires a mild pressure of ~0.3 kbar to become superconducting with T_c=12.8 K [4]. The iodide analog, κ-$(ET)_2Cu[N(CN)_2]I$, is an insulator at low temperature even under applied pressures up to 5 kbar [5]. It is isostructural with the chloride and bromide salts except for the presence of crystallographic disorder due to two ethylene group conformations observed for the ET molecules [6].

A property that is common to all the κ-phase superconductors is an unusual peak in the resistivity at

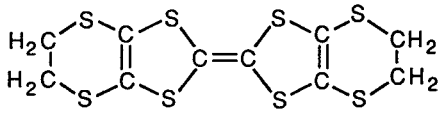

Scheme 1.

100 K. Thus, upon cooling from room temperature, these materials are initially slightly metallic, then become semiconducting down to about 100 K, where they begin to become highly metallic before the transition to superconductivity at around 10 to 13 K. In the case of κ-$(ET)_2Cu(NCS)_2$ (T_c=10.4 K), it has been shown that the resistivity peak can be reduced and the semiconducting phase suppressed by the application of pressure [7].

Another important feature common to ET-based superconductors is the possible presence of conformational disorder and its effect on T_c [1]. The two terminal ethylene groups in the ET molecule are twisted out of the molecular plane, so that, depend-

ing on whether the ethylene groups are twisted in the same or different directions, the ET molecules have an eclipsed or staggered conformation, respectively, when viewed along the central C=C bond. For β-$(ET)_2I_3$, under ambient pressure the structure is modulated (due to an ethylene group disorder) and $T_c=1.5$ K, whereas at $P=0.5$ kbar the structure becomes ordered and $T_c=8$ K [8]. The κ-phase superconducting salts exhibit disorder at room temperature due to the random occurrence of both ethylene group conformations [6,9]. At low temperatures, the ET molecules order, resulting in superconductivity, except in the case of κ-$(ET)_2Cu[N(CN)_2]I$, which remains disordered at low temperature and does not become superconducting [6].

In this paper we describe our investigation of the pressure dependence of the structure of κ-$(ET)_2Cu[N(CN)_2]Cl$. Pressure was applied by use of a diamond anvil cell at room temperature and by solidification of a grease coating on crystals at low temperatures. In addition to the pressure and temperature dependence of lattice parameters and peak profiles, the complete structure was determined at room temperature and 3 kbar. A reversible structural phase transition from orthorhombic to lower symmetry was observed to occur at ~8 kbar at room temperature in a diamond anvil cell and at low temperature with grease-coated crystals. It appears likely that this monoclinic or triclinic structural phase is associated with the superconducting electronic phase of κ-$(ET)_2Cu[N(CN)_2]Cl$. A second transition at ~12 kbar at room temperature is characterized by the reversible disappearance of Bragg peaks and may be due to pressure-induced amorphization [10,11].

2. Experimental

2.1. Room temperature diamond anvil cell experiments

Two flat, plate-like crystals approximately 100 μm thick were used in these experiments. The large flat face was indexed as the (101) face for one crystal (I) and the (010) face for the other (II), thus allowing us to obtain data over a larger region of reciprocal space than possible with one crystal in one orientation. Each crystal was mounted in a Merrill-Bassett-type diamond anvil cell, with mineral oil as the hydrostatic pressure medium and ruby chips as the pressure calibrant, in the manner described by Hazen and Finger [12].

2.1.1. Data collection

All intensity measurements in diamond anvil cells were made by use of a Krisel automated Huber diffractometer with monochromatized Mo Kα radiation from a conventional sealed tube X-ray source. Collection of diffraction intensities on crystal II was preceded by measurements of unit cell parameters of crystals in the diamond anvil cells at low pressure, i.e., near ambient pressure ($a=12.947(5)$, $b=29.876(8)$, $c=8.460(2)$ Å, $V=3272(2)$ Å^3), and at approximately 3 kbar ($a=12.880(2)$, $b=29.719(16)$, $c=8.420(5)$ Å, $V=3223(2)$ Å^3). Lattice parameters were obtained from the centering of up to 20 reflections, each with the eight equivalent positions of reflections with $2\theta\approx25°$ [13,14]. Bragg intensities for all accessible data within a sphere of reciprocal space out to $(\sin\theta)/\lambda=0.6$ Å^{-1} were measured for crystal II using the fixed-ϕ mode to maximize reflection accessibility and minimize attenuation by the diamond cell [15]. Omega step scans of 0.04° increments and 8 second counting times were used.

Upon completion of data collection for II, crystal I, mounted in a second diamond anvil cell, was pressurized so that its ruby fluorescence matched that of II. Once on the diffractometer, the pressure of crystal I was further adjusted so that the lattice parameters obtained from I ($a=12.877(5)$, $b=29.711(4)$, $c=8.423(5)$ Å, $V=3223(2)$ Å^3) were within 1σ of those from II, indicative that the pressures of the two crystals were nearly identical. Intensity data collection of the accessible hemisphere of reciprocal space were obtained from I in the manner described for II.

The data for each scan were converted to integrated intensities by application of the Lehman and Larson algorithm [16] except in some cases where the manual selection of backgrounds was necessary. Corrections were made for Lorentz and polarization effects, crystal absorption and absorption by the diamond and Be components of the pressure cell [12]. Standard reflections which were measured periodically exhibited a precipitous 40% decrease in inten-

sity about half-way through the crystal I data collection. Attempts to restore the intensities of the standards by recentering were not successful. Since the peak shapes remained good and their intensities stabilized, data collection was continued. The data were normalized by fitting the fall-off in the intensities of the standards to a series containing two exponential terms and a linear term. The subsequent averaging of equivalent reflections for crystal I produced $R(I)=0.041$ and $R_w(I)=0.028$ for 435 means based on 1998 reflections ($I \gtrsim 3\sigma$). Thus, the fall-off in the intensities of the standards is not the result of a structural phase transition or an inherent change in the crystal.

The data from crystals I and II were independently used to refine a model with initial atomic coordinates from the ambient pressure structure of κ-$(ET)_2Cu[N(CN)_2]Cl$ [6]. By use of the scale factors from these refinements, the data from each crystal were first scaled to an absolute level, then combined and averaged ($R(I)=0.041$, $R_w(I)=0.029$, for $I \gtrsim 3\sigma$) to yield a total of 918 independent reflections with $F_o^2 > 3\sigma(F_o^2)$. The final least squares refinements, including corrections for anomalous dispersion and extinction, are based on 775 reflections due to the rejection of outliers if $|w(F_o - F_c| > 10.0$, if $F_o > 2F_c$ (i.e., $I_o > 4I_c$), or if the extinction was greater than 30%. The rejection of ~15% of the data on the first two criteria is justified by examination of their peak profiles which exhibit poor shapes, difficult-to-define backgrounds and overlap problems with scattering from the diamond anvil cell. Data collection and refinement parameters are listed in table 1. The atomic positional and isotropic thermal parameters are given in table 2.

2.1.2. Unit cell parameters versus pressure

Unit cell parameters of crystals I and II were determined at several pressures to 11.4 kbar using a Picker automated diffractometer with Nb-filtered Mo Kα radiation. In addition to the eight-reflection centering procedure noted above, we employed an improved peak profile algorithm that adjusts for the separation and relative intensities of $K\alpha_1$ and $K\alpha_2$ contributions to the diffraction peaks. Unit cell parameters at several pressures are given in table 3 and are plotted in fig. 1. Note that peaks broaden and intensities decrease significantly above about 8 kbar as shown in fig. 2. At 11.8 kbar Bragg maxima disappear completely, but reappear reversibly upon lowering pressure.

2.2. Cooling grease-coated crystals

It had been demonstrated previously [5] that coating a crystal with Apiezon N grease or GE varnish, followed by cooling, would provide sufficient applied pressure to the crystal to produce the superconducting state at low temperature, whereas cooling without an applied stress such as that from grease leads to a weakly ferromagnetic insulating state [17]. In an initial attempt to investigate the possible structural effects associated with these observations, grease-coated crystals were cooled from room temperature to 15 K on a single crystal X-ray diffractometer equipped with a closed-cycled helium Displex refrigerator. It was observed that peaks that were sharp and single at room temperature were broad at low temperature, with an order of magnitude reduction in peak height. Upon warming to room temperature, the peaks sharpened and regained their previous intensities.

In order to investigate the temperature dependence of the peak shapes, scans were measured on an X-ray diffractometer equipped with a nitrogen gas cold stream apparatus capable of cooling to 110 K, since centering the crystal at each temperature is very time-consuming with the crystal mounted in the Displex. The results of cooling and then slowly warming a grease-coated, small, plate-like crystal are shown in fig. 3. No peak broadening effects were observed when this same crystal was cooled before being coated with grease. With large, block-shaped crystals, the effects of the grease were found to be small (50% peak broadening) or unobservable. However, in all cases, observable effects were reversible upon warming.

3. Results and discussion

3.1. Structural phase transitions

X-ray diffraction evidence for two high-pressure structural phase transitions, one at 8.8 kbar and one at 11.4 kbar, is obtained from single crystals of κ-$(ET)_2Cu[N(CN)_2]Cl$ in diamond anvil cells at

Table 1
Unit cell, data collection and refinement parameters for κ-$(ET)_2Cu[N(CN)_2]Cl$ at room temperature and $P=3$ kbar

Temperature	298 K
Pressure	2.9(5) kbar
Space group	Pnma
Z	8
a	12.903(2) Å
b	29.785(4) Å
c	8.431(2) Å
V	3242.2(7) Å^3
X-radiation	Mo Kα, $\lambda=0.7107$ Å
Data collection	ω scans, 2 crystals in 2 diamond anvil cells
Absorption coefficient μ	8.989 cm^{-1}
No. of unique refls. in final l.s.	775
No. of variables	95
Extinction g [a)]	0.024(5) rad^{-1} 10^{-4}
$R(F)=\Sigma\|F_o-F_c\|/\Sigma\|F_o\|$	0.116
$R_w(F)=[\Sigma w(F_o-F_c)^2/\Sigma wF_o^2]^{1/2}$	0.108
GOF$=[\Sigma w(F_o-F_c)^2/(NO-NV)]^{1/2}$	3.13

a) Becker and Coppens lorentzian mosaic spread distribution [20].

Table 2
Positional and isotropic thermal parameters for κ-$(ET)_2Cu[N(CN)_2]Cl$ at room temperature and $P=3$ kbar

Atom	x	y	z	U (Å^2) [a)]
Cu	0.3658 (5)	0.25	0.5686(8)	0.038(2)
Cl	0.3544(9)	0.25	0.8265(16)	0.039(4)
N(0)	0.0523(33)	0.25	0.3524(55)	0.053(15)
N(1)	0.2255(29)	0.25	0.4619(47)	0.040(13)
N(2)	−0.0183(34)	0.25	0.0860(59)	0.061(16)
C(11)	0.1448(45)	0.25	0.3881(66)	0.060(20)
C(12)	0.0143(37)	0.25	0.2093(70)	0.043(17)
S(1)	−0.0291(6)	0.5232(4)	0.2671(11)	0.028(3)
S(2)	0.0978(6)	0.5659(3)	0.0234(10)	0.021(3)
S(3)	0.1157(6)	0.4365(3)	0.2694(11)	0.030(3)
S(4)	0.2472(7)	0.4742(4)	0.0186(11)	0.030(3)
S(5)	−0.1528(7)	0.6021(3)	0.3391(12)	0.036(3)
S(6)	0.0018(7)	0.6538(4)	0.0457(12)	0.047(3)
S(7)	0.2324(7)	0.3535(4)	0.3043(12)	0.037(3)
S(8)	0.3868(7)	0.3971(3)	−0.0030(12)	0.041(3)
C(1)	0.0789(18)	0.5204(11)	0.1412(34)	0.006(8)
C(2)	0.1367(22)	0.4835(11)	0.1479(36)	0.020(9)
C(3)	−0.0539(22)	0.5810(12)	0.2271(41)	0.031(11)
C(4)	0.0039(22)	0.5970(12)	0.1059(39)	0.024(10)
C(5)	0.2174(21)	0.4054(11)	0.2093(38)	0.022(9)
C(6)	0.2739(21)	0.4190(11)	0.0877(37)	0.015(9)
C(7)	−0.1754(27)	0.6544(15)	0.2613(48)	0.064(14)
C(8)	−0.0858(23)	0.6746(12)	0.2003(40)	0.037(11)
C(9)	0.3180(23)	0.3229(12)	0.1630(43)	0.039(11)
C(10)	0.4123(20)	0.3491(10)	0.1218(33)	0.007(8)

a) Isotropic temperature factors of the form $\exp(-B(\sin^2\theta)/\lambda)$, where $B=8\pi^2U$.

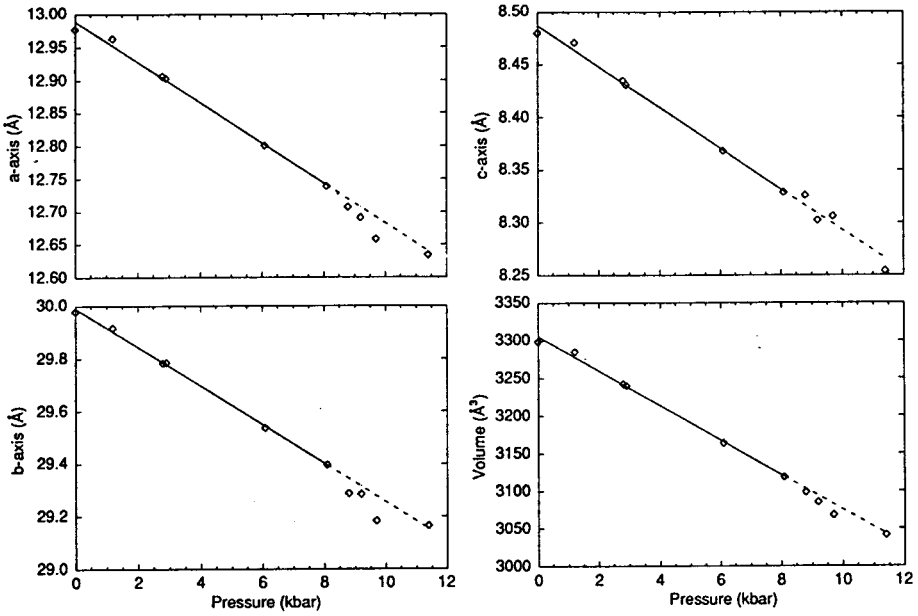

Fig. 1. Unit cell parameters of κ-$(ET)_2Cu[N(CN)_2]Cl$ as a function of pressure at room temperature. The solid lines are based on data with $0 \leq P \leq 8.1$ kbar (see text) and are extended to higher pressures with dashed lines.

Table 3
Unit cell parameters of κ-$(ET)_2Cu[N(CN)_2]Cl$ at several pressures

I. Orthorhombic phase Pnma (No. 62), $Z=4$

P (kbar)	a (Å)	b (Å)	c (Å)	V (Å³)	V/V_0	Crystal
0	12.977(3)	29.979(4)	8.480(2)	3299.0(12)	1.0	[a]
1.2(4)	12.963(2)	29.917(2)	8.471(2)	3285.2(8)	0.996	II
2.8(6)	12.906(2)	29.783(1)	8.435(2)	3242.2(7)	0.983	I
2.9(5)	12.903(2)	29.785(4)	8.431(2)	3240.3(9)	0.982	II
6.1(6)	12.801(1)	29.537(1)	8.368(2)	3164.0(5)	0.959	I
8.1(5)	12.739(2)	29.397(4)	8.329(2)	3118.9(8)	0.945	II [b]

II. Pseudo-orthorhombic phase [c]

P (kbar)	a (Å)	b (Å)	c (Å)	α (°)	β (°)	γ (°)	V (Å³)	V/V_0
8.8(6)	12.707(4)	29.288(6)	8.326(4)	90.01(3)	89.94(3)	89.99(2)	3098.7(20)	0.939
9.2(6)	12.691(1)	29.285(2)	8.302(1)	90.032(7)	90.027(9)	90.036(6)	3085.4(6)	0.935
9.7(4)	12.658(1)	29.184(4)	8.306(1)	90.06(1)	89.912(9)	90.076(9)	3068.2(6)	0.930
11.4(4)	12.634(3)	29.165(6)	8.254(2)	90.06(2)	90.20(2)	90.11(2)	3041.5(11)	0.922
11.8(5)				Intensities disappear reversibly				

[a] Unit cell parameters from ref. [6].

[b] At $P=8.1$ kbar, unconstrained refinement gives $a=12.739(2)$, $b=29.397(2)$, $c=8.329(2)$ Å, $\alpha=90.00(2)°$, $\beta=89.99(1)°$, $\gamma=89.98(3)°$, $V=3118.9(8)$ Å³.

[c] Above 8.1 kbar, peaks display broadening and splitting characteristic of a displacive phase transition. Peak intensities decrease and disappear reversibly above 11.8(5) kbar.

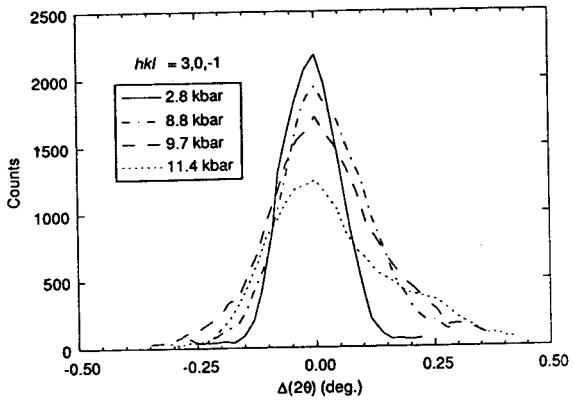

Fig. 2. The variation of peak profiles (θ–2θ scans) with pressure for the (3 0 $\bar{1}$) peak of a crystal of κ-$(ET)_2Cu[N(CN)_2]Cl$ in a diamond anvil cell at room temperature.

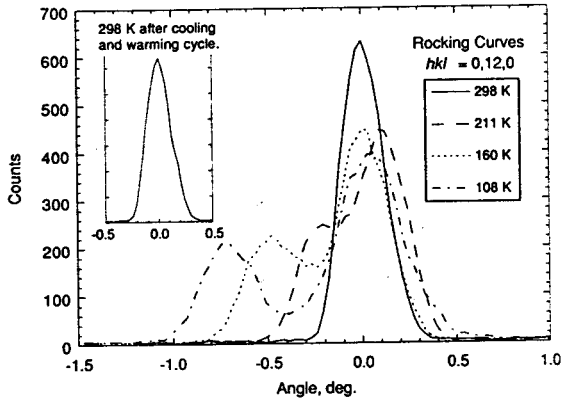

Fig. 3. Rocking curves (ω scans) as a function of temperature for the (0 12 0) peak of a crystal of κ-$(ET)_2Cu[N(CN)_2]Cl$ coated with Apiezon N grease. The crystal was cooled from room temperature to 108 K. The insert shows the peak has regained its shape and intensity after warming back to room temperature.

room temperature. Up to 8.1 kbar, the X-ray diffraction Bragg peaks are sharp. At 8.8 kbar and above, the peaks broaden and intensities begin to drop. As shown in fig. 2, the (3 0 $\bar{1}$) intensity goes from about 2200 cps below 8 kbar, to 1900, 1700, and 1200 at 8.8, 9.7, and 11.4 kbar, respectively. Similarly, the (0 12 0) intensity goes from about 4000 cps below 8 kbar, to below 1500 cps at 11.4 kbar. These changes are accompanied by significant peak broadening in θ–2θ scans, as shown in fig. 2.

A similar effect was observed when cooling crystals coated with Apiezon N grease, which apparently hardens and applies pressure sufficient for obtaining the superconducting state at low temperature [5]. As shown in fig. 3 for the (0 12 0) peak, the peak broadening and the appearance of multiple peaks is reversible upon warming. For the same crystal, distinct multiple peaks were also observed at low temperatures in scans of the (8 0 0) reflection, whereas the (0 0 4) peak simply broadened.

These observations are consistent with a transition from the low pressure orthorhombic phase to a high pressure phase of monoclinic or triclinic symmetry. The peak broadening at elevated pressure is then due to the presence of multiple domains with symmetry-lowering distortions in different directions. Multidomain structures are common to the high-T_c copper oxide superconductors due to tetragonal to orthorhombic transitions upon cooling, but this type of multidomain structure in the superconducting state is *unique* to κ-$(ET)_2Cu[N(CN)_2]Cl$ among the ET-based superconductors. The deviations from 90° of the unit cell angles derived from data with $P \geq 8.8$ kbar appear to be real (table 3). For $P \leq 8.1$ kbar, the angles from unconstrained refinements are all within 1σ and 0.02° of 90.00° (table 3, footnote b)).

Examination of table 3 and fig. 1 in the pressure range of 8.8 to 9.7 kbar indicates higher compressibilities for the *a*- and *b*-axes relative to those at lower pressures and to the *c*-axis. Then, from 9.7 to 11.4 kbar, the *a*- and *b*-axes remain relatively constant while the *c*-axis continues to decrease in length. Multiple displacive transitions with pressure in the triclinic domain are known to exist in many compounds [18] and further investigations are underway to clarify the behavior of possible multiple changes in κ-$(ET)_2Cu[N(CN)_2]Cl$ at pressures above 8 kbar.

A different type of phase transition occurs between 11.4 and 11.8 kbar. This transition is characterized by the completely reversible disappearance of Bragg reflections at 11.8 kbar, which reappear at lower pressures without loss of crystallinity. It is possible that this transition is related to the class of transitions known collectively as "pressure-induced amorphization", examples of which include quartz, ice, calcium hydroxide, and $AlPO_4$ or berlinite [10,11]. In the case of single crystals of AlPO4, wher the pressure is reduced, the high pressure amorphou

material transforms back to a single crystal with the same orientation as the starting crystal [10]. The proposed explanation for this unusual phenomenon is that at elevated pressure the atoms or molecules are randomly displaced by small amounts from their ordered positions, so that they easily return to the previous crystalline state upon decompression. Further studies on κ-$(ET)_2Cu[N(CN)_2]Cl$ in the pressure range 8 to 12 kbar are in progress.

3.2. Linear compressibilities and bulk modulus

The unit cell parameters of κ-$(ET)_2Cu[N(CN)_2]Cl$ at several pressures up to ~12 kbar are tabulated in table 3 and plotted in fig. 1. However, since the Bragg peaks display broadening and splitting above 8.1 kbar, only lattice parameters in the range $0 \leq P \leq 8.1$ kbar were used to obtain compressibilities. The pressure dependence of the unit cell parameters were fit to the expression

$$p = p_0 - d_1 P + d_2 P^2 ,$$

where p_0 is the value of the lattice parameter with zero applied pressure, P is the pressure in kbar, and d_1 and d_2 are fitted parameters. For each of the unit cell parameters for κ-$(ET)_2Cu[N(CN)_2]Cl$, including the unit cell volume, the d_2 parameter is not significant and the temperature dependence is linear:

$$a = 12.989(6) - 0.031(1)P ,$$

$$b = 29.992(7) - 0.074(2)P ,$$

$$c = 8.487(3) - 0.0194(8)P ,$$

$$V = 3306(3) - 23.0(7)P .$$

The ambient pressure linear compressibilities ($\beta = d_1/p_0$) are $\beta_a = 2.39(8) \times 10^{-3}$, $\beta_b = 2.47(7) \times 10^{-3}$ and $\beta_c = 2.29(9) \times 10^{-3}$ $kbar^{-1}$. Considering the two-dimensional layered nature of the κ-$(ET)_2Cu[N(CN)_2]Cl$ structure (figs. 4 and 5), the highly isotropic compressibilities (0.97:1.0:0.93) are surprising. In the case of κ-$(ET)_2Cu(NCS)_2$, the observed anisotropy of the principal compressibilities (4.7×10^{-3}, 2.5×10^{-3}, and 0.8×10^{-3} $kbar^{-1}$) is in the ratio (1:0.53:0.17), with the smallest compressibility parallel to the long axis of the ET molecule [19]. These results are surprising because both types of salts have similar layered structures, although there are important differences which are discussed in the following section. The ambient pressure bulk modulus $K = \beta_{\bar{V}}^{-1}$ is 144(4) kbar for κ-$(ET)_2Cu[N(CN)_2]Cl$, which compares to a value of 122 kbar for κ-$(ET)_2Cu(NCS)_2$ [19]. Thus, κ-$(ET)_2Cu[N(CN)_2]Cl$ is slightly less compressible than is κ-$(ET)_2Cu(NCS)_2$.

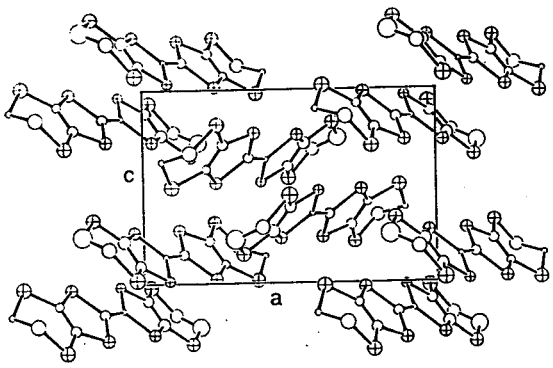

Fig. 4. The ET molecule layer centered at $y=0$ of κ-$(ET)_2Cu[N(CN)_2]Cl$ at 3 kbar and room temperature. Atoms are drawn at the 50% probability level. Carbon atoms are drawn with open circles and sulfur atoms with cross-hatched circles.

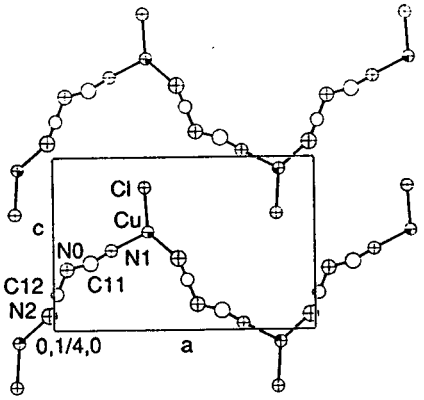

Fig. 5. The $\{Cu[N(CN)_2]Cl^{1-}\}_n$ anion layer at $y=\frac{1}{4}$ of κ-$(ET)_2Cu[N(CN)_2]Cl$ at 3 kbar and room temperature. Atoms are drawn at the 50% probability level. The anions form infinite polymeric chains in the a-axis direction. Anion and ET layers (fig. 4) alternate in the b-axis direction.

3.3. High pressure crystal structure

As shown in figs. 4 and 5, the structure of κ-$(ET)_2Cu[N(CN)_2]Cl$ consists of ET layers sandwiched between layers of the polymeric anion $\{Cu[N(CN)_2]Cl^{-1}\}_n$. The packing motif in the ET layers consists of face-to-face ET dimers with nearest neighbor dimers arranged orthogonally, which is characteristic of κ-type structures. There are two layers per unit cell with successive layers related by mirror planes in which the anions reside. The long axes of the ET molecules are not parallel to the *b*-axis but tilt in a direction parallel to the polymeric anion chains along the *a*-axis direction.

One of the questions we wished to investigate was whether at 3 kbar the ET molecules retain their eclipsed conformation which exists at ambient pressure. That is, when viewed along the central C=C double bond, the terminal ethylene groups appear either eclipsed or staggered relative to each other depending on the displacements of the ethylene carbon atoms above and below the molecular ET plane. As seen in fig. 4, the ET molecules do retain the eclipsed conformation at 3 kbar. It is of interest to note that in κ-$(ET)_2Cu(NCS)_2$ (T_c=10 K), the ET molecules have a staggered conformation, there is one layer per unit cell, and the ET molecules tilt in a direction which is perpendicular to the $\{Cu(NCS)_2^{-1}\}_n$ polymeric chains [9].

Due to the lack of sufficient data, it is difficult to characterize with a high degree of precision subtle changes in the conformation or packing between the low and high pressure structures. At this intermediate pressure, which is well below the 8 kbar transition, there is no evidence of any dramatic change in the structure. However, intermolecular S···S contacts at or near the sum of the van der Waals radii of 3.60 Å, which provides the electron conduction pathway in ET-based metals, are compared for ambient pressure and 3 kbar at room temperature in table 4. As can be seen, many of these contacts are reduced by 0.05 Å or more. The shortest intermolecular contact, S(5)···S(7), reduces from 3.489(2) Å at ambient pressure to 3.44(1) Å at 3 kbar.

Table 4
Intermolecular S···S contacts in κ-$(ET)_2Cu[N(CN)_2]Cl$ at room temperature

Atoms	P=1 bar [a]	P=3 kbar [b]
S(1)···S(8)	3.598(2)	3.57(1)
S(1)···S(4)	3.722(2)	3.70(1)
S(1)···S(2)	3.740(2)	3.71(1)
S(1)···S(4)	3.766(2)	3.70(1)
S(2)···S(5)	3.615(2)	3.58(1)
S(2)···S(3)	3.727(2)	3.70(1)
S(2)···S(7)	3.796(2)	3.73(1)
S(3)···S(5)	3.570(2)	3.52(1)
S(3)···S(8)	3.784(2)	3.73(1)
S(3)···S(4)	3.854(2)	3.82(1)
S(4)···S(5)	3.983(2)	3.96(2)
S(5)···S(7)	3.489(2)	3.44(1)
S(5)···S(8)	3.715(2)	3.68(1)

[a] Ref. [6].
[b] This work.

4. Conclusions

A reversible pressure-induced structural phase transition, that we believe is associated with the pressure-induced superconducting state of κ-$(ET)_2Cu[N(CN)_2]Cl$, has been studied. The evidence for this symmetry-lowering transition is the broadening and splitting of Bragg peaks at ~8 kbar and room temperature. This same behavior is observed upon cooling crystals coated with Apiezon N grease, which is a procedure that has been shown to produce the superconducting state in κ-$(ET)_2Cu[N(CN)_2]Cl$ at low temperature (T_c=12.8 K, P=0.3 kbar). A second transition at ~12 kbar results in the reversible disappearance of Bragg reflections which is characteristic of pressure-induced amorphization. Another interesting finding is the isotropic character of the linear compressibilities of κ-$(ET)_2Cu[N(CN)_2]Cl$, which would seem to be unusual for a layered structure of this type, which may indicate greater three-dimensionality than implied by the two-dimensional structural motif. Finally, at 3 kbar and room temperature the intermolecular S···S contacts are as much as 0.05 Å less than those at ambient pressure.

Acknowledgements

Work at Argonne National Laboratory is supported by the Office of Basic Energy Sciences, Division of Materials Sciences, US Department of Energy, under Contract W-31-109-ENG-38. Crystallographic studies at the Geophysical Laboratory were supported by NSF grant EAR921 8845.

References

[1] J.M. Williams, A.J. Schultz, U. Geiser, K.D. Carlson, A.M. Kini, H.H. Wang, W.-K. Kwok, M.-H. Whangbo and J.E. Schirber, Science 252 (1991) 1501.

[2] J.M. Williams, J.R. Ferraro, R.J. Thorn, K.D. Carlson, U. Geiser, H.H. Wang, A.M. Kini and M.-H. Whangbo, Organic Superconductors (Including Fullerenes): Synthesis, Structure, Properties and Theory (Prentice Hall, New Jersey, 1992).

[3] A.M. Kini, U. Geiser, H.H. Wang, K.D. Carlson, J.M. Williams, W.K. Kwok, K.G. Vandervoort, J.E. Thompson, D.L. Stupka, D. Jung and M.-H. Whangbo, Inorg. Chem. 29 (1990) 2555.

[4] J.M. Williams, A.M. Kini, H.H. Wang, K.D. Carlson, U. Geiser, L.K. Montgomery, G.J. Pyrka, D.M. Watkins, J.M. Kommers, S.J. Boryschuk, A.V. Strieby Crouch, W.K. Kwok, J.E. Schirber, D.L. Overmyer, D. Jung and M.-H. Whangbo, Inorg. Chem. 29 (1990) 3272.

[5] H.H. Wang, K.D. Carlson, U. Geiser, A.M. Kini, A.J. Schultz, J.M. Williams, L.K. Montgomery, W.K. Kwok, U. Welp, K.G. Vandervoort, S.J. Boryschuk, A.V. Strieby Crouch, J.M. Kommers, D.M. Watkins, J.E. Schirber, D.L. Overmyer, D. Jung, J.J. Novoa and M.-H. Whangbo, Synth. Met. 42 (1991) 1983.

[6] U. Geiser, A.J. Schultz, H.H. Wang, D.M. Watkins, D.L. Stupka, J.M. Williams, J.E. Schirber, D.L. Overmyer, D. Jung, J.J. Novoa and M.-H. Whangbo, Physica C 174 (1991) 475.

[7] W. Kang, D. Jérome, C. Lenoir and P. Batail, J. Phys. Condens. Matt. 2 (1990) 1665.

[8] A.J. Schultz, H.H. Wang, J.M. Williams and A. Filhol, J. Am. Chem. Soc. 108 (1986) 7853.

[9] A.J. Schultz, M.A. Beno, U. Geiser, H.H. Wang, A.M. Kini, J.M. Williams and M.-H. Whangbo, J. Solid State Chem. 94 (1991) 352.

[10] M.B. Kruger and R. Jeanloz, Science 249 (1990) 647.

[11] S.K. Sikka and S.M. Sharma, Current Science 63 (1992) 317.

[12] R.M. Hazen and L.W. Finger, Comparative Crystal Chemistry (Wiley, New York, 1982).

[13] W.C. Hamilton, in: International Tables for X-Ray Crystallography, vol. 4, eds. J.A. Ibers and W.C. Hamilton (Kynoch, Birmingham, England, 1974) p. 273.

[14] H.E. King and L.W. Finger, J. Appl. Crystallogr. 12 (1979) 374.

[15] L.W. Finger and H.E. King, Am. Mineral. 63 (1978) 337.

[16] M.S. Lehman and F.K. Larsen, Acta Crystallogr. A 30 (1974) 580.

[17] U. Welp, S. Fleshler, W.K. Kwok, G.W. Crabtree, K.D. Carlson, H.H. Wang, U. Geiser, J.M. Williams and V.M. Hitsman, Phys. Rev. Lett. 69 (1992) 840.

[18] R.M. Hazen and L.W. Finger, Phase Transitions 1 (1979) 1.

[19] D. Chasseau, J. Gaultier, M. Rahal, L. Ducasse, M. Kurmoo and P. Day, Synth. Met. 41–43 (1991) 2039.

[20] P.J. Becker and P. Coppens, Acta Crystallogr. A 30 (1974) 129.